JOURNAL OF GEOPHYSICAL RESEARCH, VOL. 102, NO. D4, PAGES 4343–4352, FEBRUARY 27, 1997

Sun photometric measurements of atmospheric water vapor column abundance in the 940-nm band

Rangasayi N. Halthore

Department of Applied Science, Brookhaven National Laboratory, Upton, New York

Thomas F. Eck

Hughes-STX Corporation, Lanham, Maryland

Brent N. Holben and Brian L. Markham

Laboratory for Terrestrial Physics, NASA Goddard Space Flight Center, Greenbelt, Maryland

Abstract. Sun photometers operating in the strong water vapor absorption 940-nm combination-vibrational band have been used to determine water column abundance in the atmosphere when the path to the Sun is clear of clouds. We describe a procedure to perform a rapid determination of the water column abundance, using sun photometers with an accuracy that is easily comparable to that of the radiosondes. The effect of parameters, such as filter bandwidth, atmospheric lapse rate, and the water vapor amount, on the accuracy of the retrieved abundance is examined. It is seen that a narrow filter band of approximately 10-nm bandwidth, positioned at the peak of absorption, is quite insensitive to the type of atmosphere present during calibration or measurement with less than 1% variability under extreme atmospheric conditions. A comparison of the retrieved water column abundance using sun photometers with contemporaneously measured values using radiosondes and microwave radiometers shows that the latest version of the radiative transfer algorithm used in this procedure, MODTRAN-3, gives far superior results in comparison with earlier versions because of the use of improved absorption coefficients in the 940--nm bands. Results from a network of sun photometers spread throughout the globe will be discussed.

Introduction

In order to adequately model processes that affect global climate it is necessary to frequently measure the distribution in the atmosphere of greenhouse gases such as water, carbon dioxide, and methane. Such data are also required to study biospheric-atmospheric interactions where these gases play an important role. Since many of the greenhouse gases interact with the visible, near-IR, and thermal IR radiation, the gaseous abundance must be known accurately for atmospheric correction of remotely sensed surface data. A topic of current interest, that is the estimate of the magnitude of clear and cloudy sky absorption of shortwave radiation (see for example, *Wiscombe* [1996]), also requires an accurate estimate of the abundance of water vapor and other gases.

Because of the ease with which sun photometers can be deployed in the field they have been increasingly used to measure atmospheric transmission in the visible and near IR and thereby estimate the aerosol optical thickness and column abundance of gases such as ozone and water vapor in the atmosphere. No doubt they provide a column-averaged value of these quantities as opposed to detailed measurements as a function of height that can be obtained by radiosondes, but the main advantage is one of simplicity and, when possible, high temporal resolution. For this reason we have been using sun photometers to measure the column water abundance, utilizing the 940-nm overtone and combination-vibrational band (201→ 000 and others). Note that sun photometers have the potential to give an independent measure of the water column abundance if it can be shown that the response of the instrument is relatively insensitive to the atmospheric lapse rate (pressure versus temperature) but sensitive to the water column abundance. This criterion contrasts with the need to calibrate other devices such as the Raman lidar and the microwave radiometer against radiosonde measurements.

Thome et al. [1992] summarize early work starting from 1912 relating transmission in water absorption bands to water column abundance. The relationship was seen to approximate a square root dependence in the strong bands [*Goody*, 1964] although significant departures were observed [*Pitts et al.*, 1977]. *Volz* [1974] describes a handheld sunphotometer operating in the 940-nm band and applies what eventually came to be known as the modified Langley method (MLM) to obtain precipitable water (PW). He used a square root law dependence, as did *Reagan et al.* [1987], who applied the same method (see below) to relate

Paper number 96JD03247.
0148-0227/97/96JD-03247$09.00

surface irradiance measurements to exo-atmospheric solar irradiance in strongly absorbing bands including the 940-nm band. A variant of this method was applied [*Reagan et. al.*, 1992] to determine atmospheric water vapor column abundance, using solar radiometers by simultaneously measuring differential solar transmission in two bands, on and near the 940-nm band. Comparisons with microwave measurements [*Reagan et al.*, 1995] indicate agreement to 5% to 10% with the solar radiometer derived values consistently lower. An error analysis by *Reagan et al.* [1992] indicated that calibration uncertainty in zero air mass voltages using the MLM was the largest single source of error (approximately 5%). *Thome et al.* [1992] describe a method based on an in-house-developed radiative transfer model to relate a solar radiometer measured water transmission in the 940-nm band determined by the MLM to PW. They also compare the results of this method with actual radiosonde measurements and some empirical techniques to report agreement to better than 10%. The non-square root dependence of optical thickness on the column abundance was explored by *Bruegge et al.* [1992] and *Halthore et al.* [1992] who modeled water vapor transmission as a function of water vapor content in the form used in this paper. *Bruegge et al.* obtained a 10% agreement with radiosonde-determined values, but the agreement is suspect, since they used the water column abundance values output by LOWTRAN-7 [*Kneizys et al.*, 1988], which is distinct from the actual water (vertical) column abundance (PW). [See also *Schmid et al.*, 1996.] *Michalsky et al.* [1995] and *Shiobara et al.* [1996] also employed the technique used by *Bruegge et al.* [1992] and *Halthore et al.* [1992] to derive water column abundance. Michalsky et al. used MODTRAN-2, a moderate wavelength resolution (2 cm^{-1}) radiative transfer program, to infer precipitable water from the 940-nm band using measurement made with a multifilter rotating band shadow band radiometer (MFRSR). Comparisons with microwave radiometer measurement resulted in rms differences of 12%. *Shiobara et al.* [1996] used a sunphotometer operating in the 940-nm band to derive equivalent water vapor amounts, using LOWTRAN-7 under clear-sky and cloudy conditions. Finally, *Schmid et al.* [1996] compare sun photometer-derived PW using four different radiative transfer codes with that derived from microwave radiometers, radiosondes, and Fourier transform spectrometers. It was found in this study that the PW derived by using the sunphotometer overpredicted radiosonde/microwave radiometer values by about 18-30%, 7-20% and 2-18% depending on whether LOWTRAN-7, MODTRAN-3, OR FASCOD3P (a line-by-line radiative transfer code) was used derive the relationship between transmission in the 940-nm filter band and PW.

In this paper, MODTRAN-3, the most recent version of the moderate resolution radiative transfer program, which has many improvements over the earlier versions [*Anderson et al.*, 1994], is used to derive the functional dependence of the column water abundance on the transmission in the 940-nm band. It will be shown that under certain conditions of filter position, filter width, and atmosphere the maximum errors in a column water measurement could easily exceed calibration errors. Frequently, conditions of the atmosphere on mountaintops where the sun photometers are calibrated is quite different from that during which measurements are made. A systematic study of atmospheric effects is therefore required. In addition, the spectral band profile of the 940-nm filter used in the radiometer has a significant effect on the dependence of water transmission on the abundance. A study of the effect of this dependence on the filter position is also required.

In this paper we retrieve water column abundance using a sunphotometer in the 940-nm band, and we study the effect of (1) atmosphere, (2) filter band profile, and (3) filter position on the dependence of transmission on the water column abundance and hence the accuracy of the retrieval. We also provide the necessary comparisons of sun photometer data with radiosonde and microwave data to estimate relative accuracy. We analyze the sun photometer data with the aid of an atmospheric transmission model such as MODTRAN-3 and evaluate the position and width of the 940-nm filter to obtain accurate and consistent water column abundance measurements. The results of this study have been used to analyze data from a global sun photometer network [*Holben et al.*, 1996].

Procedure

To illustrate the simple theoretical basis of water column abundance measurement (or, for that matter, any trace gas species abundance) by using sun photometers, we review the extinction laws. The amount of light extinguished during its passage through the atmosphere is directly proportional to the density (ρ), path length (x), and extinction coefficient (κ), in addition to the amount of incident light (E) itself, so that

$$\Delta E = E\kappa\rho\Delta x \tag{1}$$

Upon integrating, we get the well known Bouguer's law of extinction,

$$E = E_0 \exp\left(-\int_{z=0}^{H} \kappa\rho dz/\mu\right) = E_0 \exp(-m\tau), \tag{2}$$

where E is the irradiance at level $z=0$, E_0 is the irradiance at the top of the atmosphere at height H above ground level, τ is the optical thickness, and z is the vertical height in the atmosphere equal to μx, where x is the slant path toward the Sun with $\mu = \cos(\theta) \sim 1/m$, where θ is the solar zenith angle and m is the air mass. Bouguer's law is strictly valid for monochromatic radiation, although Bouguer himself deduced this law in 1725 for the visible part of the sunlight reflected off the moon. In the presence of strong wavelength dependent absorption (or extinction), such as in the core of spectral lines that constitute a given band, saturation occurs, and further passage through the atmosphere results in a much weaker absorption only in the pressure-broadened line wings. This results in a nonlinear dependence of extinction upon the column abundance. For example, it has been shown that in the case of an absorption band having a large number of spectral lines that can be considered to be distributed randomly within the band, the extinction depends on the square root of the column abundance w ($=\int \rho dz/\mu$). In general, the dependence of transmission T_w on the water column abundance can be written as [*Halthore et al.*, 1992; *Bruegge et al.*, 1992]

$$T_w = \exp(-am^b W^b) \tag{3}$$

where W is the vertical column abundance. "Constants" a and b depend on the wavelength position, the width and shape of the sunphotometer filter function, the atmospheric pressure-temperature lapse rate, and the vertical distribution of water vapor. For the retrieval of water column abundance using sun

photometers to be effective under a variety of atmospheric conditions, it is necessary to have a and b insensitive to those conditions. It will be shown here that by appropriately choosing the filter center wavelength and width it is possible to have a and b relatively constant under varying atmospheric conditions, thus validating the model in equation (3). The error involved will be shown to be negligible for this type of measurement.

In the 940-nm water absorption band the response V (voltage, for example) of the sun photometer to an irradiance E is given by

$$V=V_0\exp(-m\tau)T_w \quad (4)$$

where τ is the optical thickness arising from broadband continuum type extinction mainly due to Rayleigh scattering and aerosol scattering and absorption in the 940-nm band. V_0 is the voltage response of the sunphotometer for extraterrestrial solar light intensity or irradiance and is obtained through a calibration procedure that is similar but not identical to that at continuum wavelengths. For instance, substituting for T_w, the transmission due to water vapor, taking logarithms, and transposing the above equation, we get

$$\ln V+m\tau=\ln(V_0)-am^bW^b \quad (5)$$

At a mountain site, where during the times of maximum air mass (m) change, that is, during mornings and evenings, the transmission of the atmosphere can be expected to be low and, more important, constant, a plot of the left-hand side of the above equation when plotted against m^b as the x axis will yield a straight line whose y intercept is $\ln(V_0)$ and whose slope is aW^b. This is a general procedure for calibration that can be termed as modified Langley method (MLM) after *Reagan et al.* [1987], who coined the term for b=0.5. Here the "constants" a and b are known beforehand, and the aerosol optical thickness in the 940-nm band is obtained by interpolation from adjacent wavelengths where aerosols are the only other attenuator other than molecular scattering.

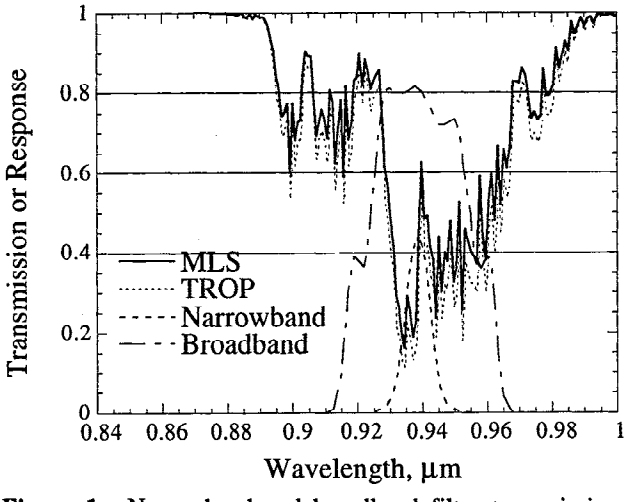

Figure 1. Narrowband and broadband filter transmissions superimposed on atmospheric water vapor transmission for midlatitude summer (MLS) and tropical (TROP) profiles as calculated by MODTRAN-3 at 10 cm^{-1} resolution. The two profiles have a water content of 2.92 cm and 4.11 cm of precipitable water, respectively.

Table 1. Transmission as a Function of Water Column Abundance for Midlatitude Summer Profile and Two Filter Bands

Zenith Angle, deg	Water Column Abundance, g/cm^2	Transmission in the Narrow Filter Band	Transmission in the Broad Filter Band
0	2.92	0.313	0.446
10	2.96	0.309	0.443
20	3.11	0.299	0.434
30	3.37	0.282	0.418
40	3.81	0.257	0.393
50	4.54	0.221	0.358
60	5.83	0.174	0.310
70	8.51	0.112	0.242
80	16.66	0.038	0.143

Optimum Choice of Filter Position and Widths

The filter position and width are determined primarily by the insensitivity of a and b in equation (5) to changes in atmospheric conditions of temperature and humidity as a function of altitude. Even though atmospheric conditions typically found in different parts of the globe can be characterized by a set of "standard" atmospheres encompassing a range of temperatures and humidities, the variability within even 1 day is considerable and therefore it is necessary to derive values of a and b in (3) that are insensitive to these changes in atmospheric conditions. In this exercise we consider only three profiles that provide the necessary range of over an order of magnitude in water column abundance: tropical (TROP), midlatitude summer (MLS), and midlatitude winter (MLW) profiles. Figure 1 shows the filter response function of two filters superimposed on the synthetic water absorption spectrum in the 940-nm band calculated by using MODTRAN-3 at a resolution of 10 cm^{-1} for the MLS and TROP profiles. For the MLS profile, vertical atmospheric water vapor transmission due to both the band and continuum absorptions are 0.313 and 0.446 for narrowband and broadband absorption, respectively. Table 1 summarizes for the MLS case, the variation in the transmission due to a variation in the water column abundance in the 940-nm band for both the narrowband and broadband filters. Variation in water column abundance is accomplished in MODTRAN-3 by keeping the temperature profile the same but by varying the zenith angle of observation. Coefficients a and b are then obtained from equation (3) by fitting a straight line for points plotted on a $\ln(\ln(1/T))$-$\ln(w)$ chart. Angles greater than 80° are not used because of the difficulty in accounting for refraction effects in the field.

From equation (3) it can be seen that a plot of $\ln(\ln(1/T))$ versus $\ln(w_{H_2O})$ from Table 1 should give a straight line whose slope is b and whose y intercept is $\ln(a)$. For each atmosphere a line fit shows that the coefficient regression is very close to 1 over a range in the abundance of over an order of magnitude. At very large zenith angles (>80°) corresponding to large values of water column abundance the coefficient of regression decreases from 1, indicating possible errors in modeling transmission as given in equation (3). In Table 2 the values of a and b are summarized for the three atmospheres taken separately and taken together. For zenith angles less than 80°, the model given in equation (3) provides a "perfect" fit for the narrow filter band, with the result that within the limits of water column abundance

Table 2. Coefficients *a* and *b* for the Narrowband and Broadband Filters for Three Standard Atmospheres Taken Separately and Together

Atmosphere	Narrowband		Broadband		W_{H_2O} range, g/cm^2
	a	*b*	*a*	*b*	
MLW	0.616	0.597	0.425	0.574	0.85-4.86
MLS	0.616	0.593	0.472	0.509	2.9-16.7
TROP	0.616	0.594	0.499	0.484	4.1-23.5
Average	0.616	0.594	0.436	0.55	0.85-23.5

Table 3. Errors in the Estimate of Water Column Abundance Given the Type of Atmosphere For Both Narrowband and Broadband Filters

Atmosphere	Narrowband	Broadband
Average	0.0	0.0
MLW	-0.75	-1.8
MLS	0.2	-3.5
TROP	-0.02	-7.1

Values are in percent.

shown the error in column abundance retrieval is independent of the magnitude. The "average" atmosphere refers to the case when all the points obtained in the three atmospheres are plotted to obtain coefficients *a* and *b*. It can be seen that while *a* and *b* are insensitive to a change in the atmosphere for the narrowband, they are quite sensitive in the broadband.

The sensitivity of the derived water column abundance to a particular type of atmosphere present during a measurement can be obtained as follows. From Table 2, if we use coefficients *a* and *b* derived for an "average" atmosphere to determine the water column abundance to be (say) 4.5 g/cm^2, corresponding to a measured transmission of 0.222 and 0.369, respectively, for the narrowband and broadband channels, then the actual water column abundance if the atmosphere were one of the three standard atmospheres would be different from the value of 4.5 g/cm^2 . The percent deviation is in Table 3. The error for the narrowband is highest for a MLW atmosphere at -0.75%, but the error for the broadband is considerably higher for a tropical atmosphere at 7.1%. The likely reason for this is that the broadband filter encompasses regions in the spectrum where the spectrally integrated absorption is temperature sensitive and modifies the transmission versus abundance relationship from that given in equation (3). Thus clearly narrowband filters (full width at half maximum of ~10-nm) must be used in sun photometers for an accurate water column abundance retrieval under varying atmospheric conditions if the transmission is modeled as given in equation (3). The error is not found to be a function of abundance, since the two-parameter model of equation (3) adequately describes the transmission within the limits of applicability as given in Table 2. Beyond these limits, deviation from the two-parameter model is seen. However, the error is in general a function of the position of the filter band. Our simulations show that for a narrowband filter at a position slightly different from that used here the errors are typically less than 1%, and therefore we suspect that the position is not as critical as the width, as long as the band encompasses a region of significant absorption.

In the above simulations, variation in abundance was obtained by changing the zenith angle for a given atmosphere, as this approach mimics the actual situation for measurements with a sunphotometer. Further simulations with a fixed zenith angle for the same atmosphere but with varying column water vapor amount showed that if PW beyond about 6 cm is used to derive *a* and *b* the values obtained will be different from those in Table 2 for the narrowband filter and about the same for the broadband filter. The reason for this discrepancy could be that saturation at large values of PW affects the narrowband transmission more than it affects the broadband transmission. Values of PW greater than 6 cm occur occasionally in the tropics, and therefore the main conclusion regarding the insensitivity of the narrowband measurements to the type of atmosphere present should be valid under most conditions.

Results

Results of comparison between sunphotometer derived water column abundance and radiosonde or microwave radiometer derived values will be discussed. Comparisons were possible because of three field campaigns, two of which were part of much larger efforts.

Wallops Island, Virginia (37°56', W75°28')

At Wallops Island, Virginia, on the Atlantic coast, a sun photometer was located within a mile of the radiosonde launch site for 16 days in July 1993. Fourteen launches coincided with a simultaneous sunphotometer measurements during clear-sky conditions. The result, plotted in Figure 2, shows that the radiosondes overpredict the sun photometer values by about

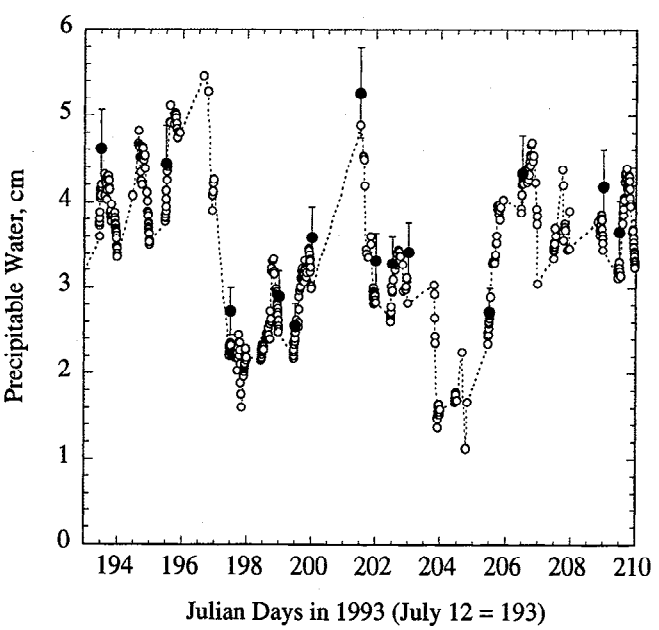

Figure 2. Comparison of radiosonde measurements of precipitable water with narrowband (940 nm) sun photometer measurements at Wallops Island, VA in July, 1993. Error bars on the radiosonde measurements depict a ±10% uncertainty. The sun photometer tends to underestimate the precipitable water by an average of 10%.

10%, the expected uncertainty of radiosonde measurements. Although it is not known what type of radiosonde was used at this site, it is our conjecture that it is one of two types [*Ferrare et al.*, 1995]: either that manufactured by Atmospheric Instrumentation Research (AIR) or that manufactured by Vaisala Corporation. The former uses a carbon hygristor to measure relative humidity, while the latter uses a thin film capacitive element. Differences of the order of 3-5% have been noted in the relative humidity derived from the two radiosondes [*Ferrare et al.*, 1995]. The seven channels of the sunphotometer spanned the wavelength region from 340 to 1030 nm with two channels, at 870-nm and 1030 nm, bracketing the narrow 940 nm channel (Figure 1), providing the necessary aerosol optical thickness by interpolation. The sun photometer, commonly known as a Cimel sunphotometer (named after the French manufacturer), was operated in the completely automatic remote mode (that is, solar tracking, data acquisition, and data transmission were all automatic) and was calibrated on Mauna Loa in Hawaii.

Radiosonde measurements provide in situ relative humidity, pressure, and temperature values as a function of height, and these are used to compute water density in grams per cubic centimeter. Integration with height provides the column abundance in grams per square centimeter, which is the same as precipitable water in centimeters. Note that it takes about one-half hour for the radiosonde to acquire all the data, although in the boundary layer, where most of the moisture is present, sampling is relatively swift soon after launch. Thus it is appropriate to plot the radiosonde values corresponding to the time at launch. The advantage of a sunphotometric measurement can be easily seen in Figure 2, in which the temporal resolution is much higher than that of the radiosonde. Diurnal variation in column moisture content is clearly seen on most days in July. Day-to-day variation depicts passage of cold fronts carrying drier air masses. On day 201 (corresponding to July 20) some of the highest values are seen in both the radiosonde and sun photometer values.

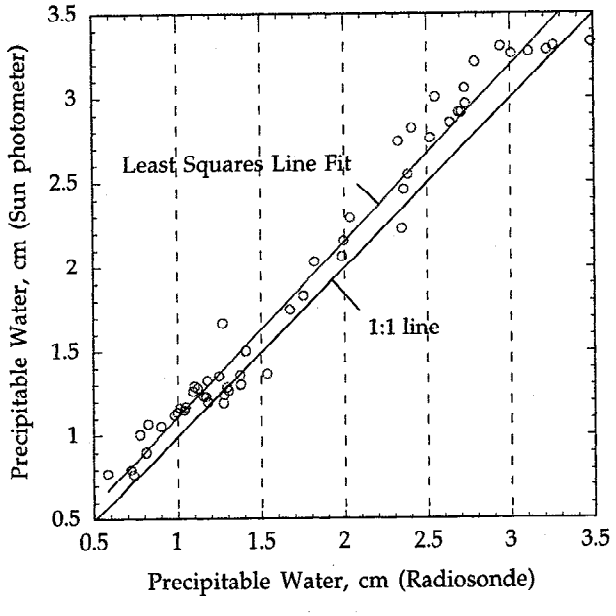

Figure 3a. Comparison of radiosonde and sun photometer measured precipitable water in April 1994 at the ARM site in Oklahoma. The sun photometer measurement was calibrated at Mauna Loa with an expected uncertainty of ±2%. Mean deviation between the two measurements is of the order of 9%, however there is a systematic effect -- the sun photometer systematically overpredicts precipitable water.

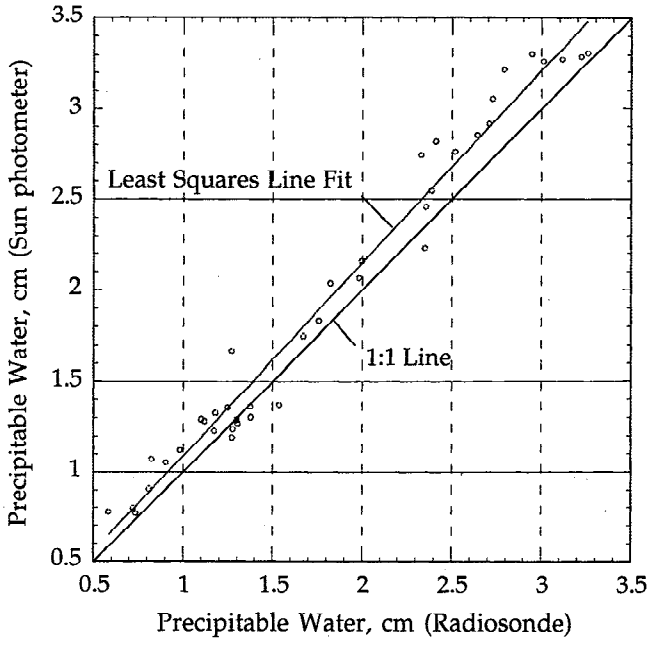

Figure 3b. Same as Figure 3a except that the sun photometer data are screened for "cloud contamination" by restricting the data set to aerosol optical thickness less than 1, Angstrom exponent to greater than 0.5, and goodness of Angstrom fit to better than 0.9 in the aerosol versus wavelength curve. The underestimate reduces to 8.5%, a negligible reduction.

Cloud and Radiation Test Bed (CART) Site (36°36', W97°24')

The CART site near Lamont, Oklahoma, is one of three primary sites chosen as part of the Department of Energy's Atmospheric Radiation Measurement (ARM) program to test global climate models by measuring the radiation components of the Earth-Atmospheric system. A sun photometer similar to the one used at Wallops Island was deployed during the intensive operations period (IOP) in April 1994 for about 3 weeks. During the IOP, radiosonde (Vaisala type) launches were more frequent, about once every 3 hours during the day. A total of 53 launches had corresponding sun photometer data. Cloud screening of the automatically processed data was done by examining the variation of aerosol optical thickness in all the channels as a function of time taken 3 at a time about 20 s apart. Optically thick clouds obscuring the Sun would prevent the automatic lock on the Sun, thus flagging the data. Optically thin cirrus clouds would be spatially inhomogeneous, thus causing variation in the three sets of data. A problem arises if cirrus clouds are present and are spatially uniform. Such data, encountered here in this data set, are usually characterized by Angstrom exponent (b in $\tau=a\lambda^{-b}$) lower than 0.5 or goodness of the Angstrom fit worse than 0.9. In Figure 3a, all the data are shown in a plot of precipitable water derived by radiosonde and by sun photometer. Here the sun photometer overestimates the PW by about 9.2%, a value close to the uncertainty in radiosonde measurements. Upon inspection of the sun photometer data it became clear that some of the data might

have been contaminated by either uniform cirrus cloud or large haze particles. In order to explore their effect, data were screened as described above, with the results plotted in Figure 3b. The overestimate reduced to about 8.5% over that of the radiosonde values. These disagreements are systematic effects, and the problem could lie in the accuracy of calibration of the sun photometer as well as bias errors in radiosonde-measured humidity.

At the CART site, precipitable water was also measured by a microwave radiometer (MWR). Although this radiometer uses radiosonde-measured precipitable water for its calibration and thus is not totally independent of radiosonde measurements, it nevertheless measures PW very frequently--every 10 min regardless of the sky condition. A large number of data points are thus available for comparison between the sun photometer and the MWR. About 500 points are shown in Figure 4a and the mean deviation is of the order of 3.5%. In Figure 4b, in which about 300 points are shown after cloud screening of the sun photometer data, the mean deviation actually increases to 5.3%! Thus, even in the presence of clouds, the water vapor abundance retrieval is accurate to the same uncertainty as that in the clear sky case. Figure 4c confirms this finding. Although most of the data were obtained in the presence of "thin" clouds, that is, clouds whose optical thickness is less than 1, some values of optical thickness exceeded 3. *Shiobara et al.* [1996] also report success in retrieving column water vapor amount in the presence of clouds, but they restrict their data to optical thickness of less than 1 and perform a correction to the measured optical thickness to account for the enhanced scattering of sunlight into the sun photometer field of view in the presence of cloud particles.

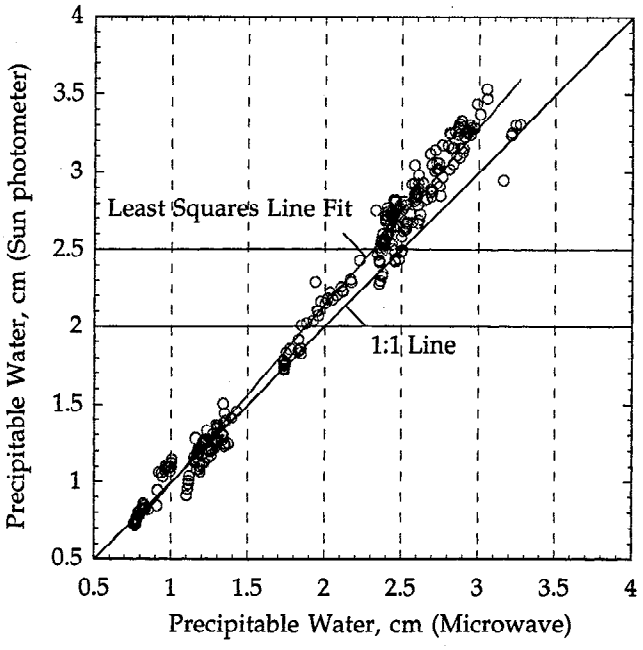

Figure 4b. Same as Figure 4a except that the sun photometer data are screened for "cloud contamination". Same criterion for data selection is used as that in Figure 3b.

The closeness of agreement with MWR is consistent with the finding of *Reagan et al.* [1987], because both methods, MWR and the sun photometer, use the similar technique of instantaneous column sampling with increased temporal resolution.

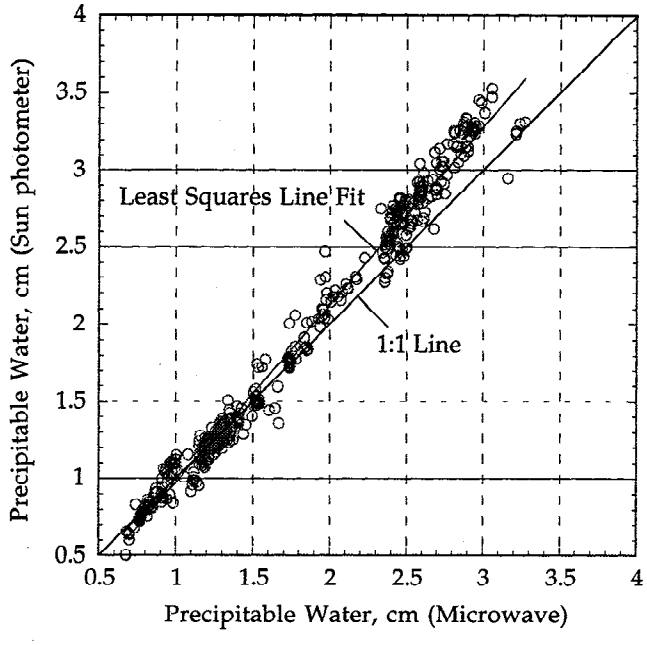

Figure 4a. Comparison between Precipitable Water measured by a Microwave Radiometer and by a narrowband sunphotometer at the Oklahoma ARM Site in April 1994. The agreement here is much better than that for radiosondes, even though the microwave radiometers are calibrated against radiosondes. This finding is perhaps due to the fact that microwave data are available more frequently than radiosondes and they represent column-averaged values, as is the case with the sun photometers. The mean deviation is of the order of ±4%.

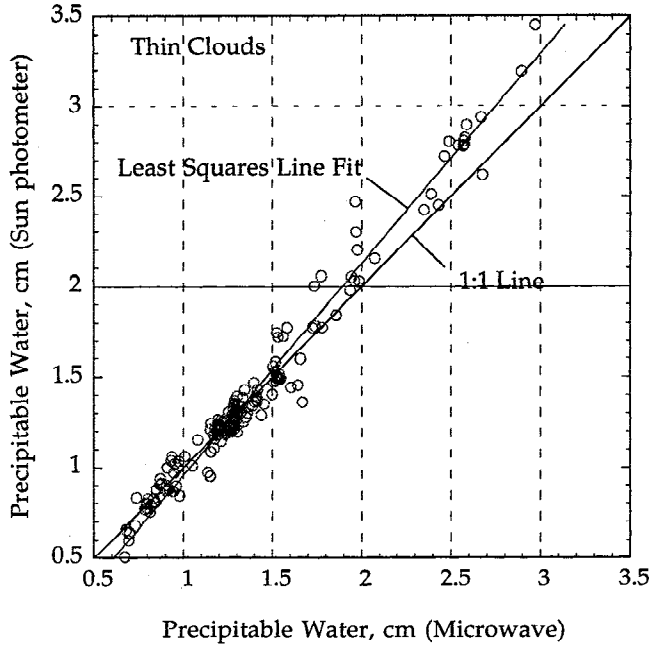

Figure 4c. Effect of clouds on the retrieval, obtained by plotting sun photometer derived values in the presence of thin clouds. The presence of thin clouds is defined by Angstrom exponent less than 0.5 and goodness of Angstrom fit poorer than 0.9. While no restrictions were placed on the optical thickness, the values were typically less than 1, with some values exceeding 3 at 440 nm.

BOREAS Southern Study Site at Candle Lake (53°43', W105°16')

The BOReal Ecosystem Atmospheric Study (BOREAS) [*Sellers et al.*, 1995] is a major effort, involving NASA and other agencies, to study the role of the boreal forest in climatic effects. Held in the north-central part of Canada, BOREAS study sites were spread over a large area stretching from Prince Albert, Saskatchewan, near the southern boundary of the boreal forest to its northern boundary near Thompson, Manitoba, about 600 km away. Because of the large extent of the site it was further divided into two: a southern study area (SSA) situated entirely in Saskatchewan and a northern study area (NSA) in Manitoba. A total of five automatic Cimel sun photometers with a narrowband 940-nm channel were deployedbetween the two study areas: three in the SSA, one in the NSA, and one in the town of Flin Flon. The strategy for this deployment and the aerosol optical thickness measurements will be discussed in a future article.

The southern study area, the results from which are presented here, spans a considerable area 100 times 100 km. During the intensive field campaigns (IFCs) a complement of three Cimel sun photometers were placed at the Prince Albert National Park (PANP) at the western end of the site, at the Young Jack Pine site (YJP) at the eastern end of the site, and at the Prince Albert Airport (PA) at the southern end. These three stations formed a triangle with sides approximately 100 km (PANP-PA) x 120 km (PANP-YJP) x 70 km. The radiosonde launches (Vaisala type) were at the BOREAS operations center (OPS) about 40 km west of the YJP site at Candle Lake. Here a NASA-built sun photometer commonly known as SXM-2 employing a broadband 940-nm channel (Figure 1) was located during the third IFC in September 1994.

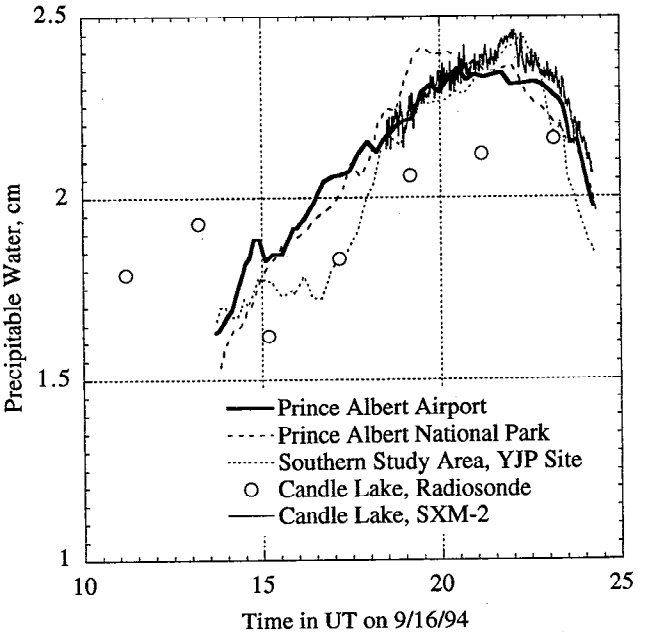

Figure 5b. Comparison of PW derived from sun photometers and radiosonde during BOREAS. SXM-2 was located at the radiosonde launch site at Candle Lake while the narrowband Cimel sun photometers were located at YJP, PANP and PA - 50 km E, 50 km W and 50 km SW from Candle Lake, respectively.

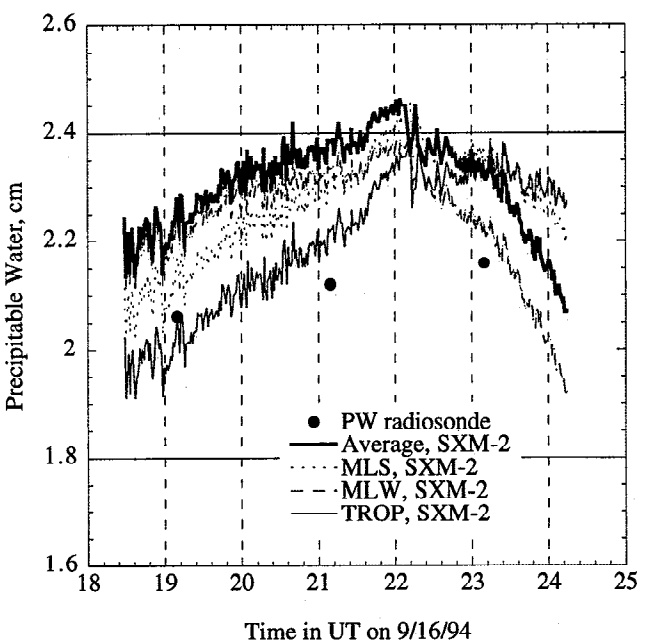

Figure 5a. Effect of uncertainty in the knowledge of the atmosphere during the time of measurement. Precipitable water (PW) derived from a radiosonde is compared with sunphotometer (SXM-2) values for four atmospheres - an "average" atmosphere, MLS, MLW and TROP. The calibration coefficient in all cases is the same and in this case is obtained from intercomparison with another sunphotometer on the same day using an "average" atmosphere. Thus the curve marked as "average" is the baseline to which other curves should be compared. The variability is seen to be of the order of 10% due to the uncertainty in the knowledge of the atmosphere.

Figures 5a and 5b depict results for September 16, a clear day with aerosol optical thickness of 0.05 at 500 nm. Three radiosonde launches (identified by filled circles in Figure 5a) at Candle Lake had a corresponding SXM-2 measured precipitable water.

Figure 5a depicts the effect of uncertainty in the knowledge of atmospheric conditions during the time of measurement. Coefficients a and b obtained for an "average" of the three atmospheric conditions, MLW, MLS, and TROP, are used to derive PW. They are obtained by intercomparison with a Cimel sun photometer on the same day at the PA airport, about 100 km away, assuming an average atmosphere. The four atmospheric conditions are then used separately to derive PW, plotted in Figure 5a. Thus the curve termed "average" in Figure 5a is probably closest to the "truth" (that is, the best possible sun photometer value), since had we used any one of the other three atmospheres during calibration and PW estimation, we would have obtained a curve close to that termed "average". Ideally, calibration at a mountain site should be performed, but this was not possible at that time. The differences of the order of 10% are clearly discernible for this broadband case. Since the broadband sun photometer is sensitive to the type of atmosphere present during the time of measurement or calibration, it cannot provide a truly independent measure of the column abundance.

In Figure 5b, radiosonde derived PW are compared with the broadband SXM-2 which is collocated at the launch site and three narrowband Cimel sun photometers located at the YJP site about 50 km east, PANP about 50 km to the west, and PA about

Table 4. Precipitable Water Around the World

Place	Type	March-May	July-October	December-February
Arizona	desert	0.83 ± 0.3	1.5 ± 0.75	0.63 ± 0.22
Thompson, Manitoba, Canada	boreal forest	1.1 ± 0.4[a]	1.6 ± 0.5	
Flin Flon, Manitoba, Canada	boreal forest	1.1 ± 0.3[a]	1.75 ± 0.55	
Prince Albert, Saskatchewan, Canada	boreal forest	1.3 ± 0.3[a] (0.4 ± 0.3)[b]	1.4 ± 0.5	
Cuiaba, Brazil	cerrado (savannah)		2.9 ± 0.9	4.7 ± 0.6
Alta Floresta, Brazil	rain forest		3.4 ± 0.9	5 ± 0.43
Maryland	urban	1.45 ± 0.6	2.8 ± 1.0	0.8 ± 0.4
Israel	desert	1.3 ± 0.4	2 ± 0.5	1.1 ± 0.4
Northern Alaska	open boreal forest	1.0 ± 0.35	1.6 ± 0.6	
Burkina Faso, Sahel	semi-desert	3.0 ± 1.0	3.9 ± 1.0 (5.5 ± 0.5)[c]	1.2 ± 0.4
Lille, France	urban	1 ± 0.4	2 ± 0.7	
Hawaii	oceanic			2.7 ± 0.6

[a]May.
[b]March.
[c]July.

60 km southwest of the launch site. The coincidence between PA and SXM-2 is not surprising, since SXM-2 was calibrated against the Cimel at PA. The disagreement between the sun photometer and the radiosonde-derived values of approximately 10% is puzzling, since it points to calibration uncertainty in the sun photometer and/or the radiosonde values. All the sun photometer data reported in this figure were analyzed with the help of calibration coefficients obtained by intercomparison with a reference sun photometer (Cimel 13) at the Goddard Space Flight Center in the months following the third IFC, in October and November. The reference sun photometer itself was calibrated at Mauna Loa on September 25 by using the MLM; its calibration coefficient is found to be consistent with that obtained on other days.. The difference between PA and SXM-2 can only be due to the spatial nonuniformity in PW.

Precipitable Water Around the World Measured With Sun Photometers

Table 4 shows the amount of precipitable water derived largely from a narrowband Cimel sun photometer network operating since 1993 [*Holben et al.*, 1996]. Since all the Cimel sun photometer derived values in this table have used coefficients using the LOWTRAN-7 code, the correct values are likely to be about 8% higher. Table 4 denotes an average PW, over 3 years in some cases, along with the square root of the variance. The values in this table should be considered as pertaining to clear-sky climatology (as opposed to cloudy skies), even though some of the data may be contaminated with thin cirrus clouds. For a discussion of the increase of PW in cloudy conditions, see *Gaffen and Elliott* [1993]. Various types of land covers are explored in this table; the surprise is the relative lack of moisture in the boreal forest of northern Canada during summer and spring. In fact, the values obtained for the boreal forest compare well with those obtained for desert and semidesert type locations such as Israel and Arizona. This finding is surprising also, since the boreal forest comprises innumerable lakes especially in the SSA, whose water temperatures reached 20°C in July (R. Halthore and B. Markham, unpublished data, 1995) and the maximum ambient temperatures recorded were more than 20°C. Dry Arctic air mass does find its way down to the BOREAS region frequently even during summer months, and that trend could partly explain the low humidity, but given the high surface and air temperature during summer months in general, an alternative explanation seems necessary.

Not surprisingly, the water vapor amount in July, measured in 1993 during a field campaign in the Sahel region of West Africa, is one of the highest values we have recorded, as July is the season of monsoon flow off the Gulf of Guinea. Figure 6 shows the results of PW measurement in all of 1995 using a sun photometer stationed in Ouagadougou, Burkina Faso. It is apparent from this figure that the year can be divided into two periods: one between March and October when the PW is about 3.5, and the rest of the year, during which PW is around 1.2 [see also *Justice et al.*, 1991, and references therein]. The Intertropical Convergence Zone (ITCZ) is to the north during summer thus establishing Hadley Cell driven southerly flow bringing in the moisture from the gulf. In the winter months the ITCZ is to the south, thus driving the dry northeasterly flow from the Sahara into the Sahel region.

In Hawaii a large number of data exist from this network but they are applicable to the top of the mountain Mauna Loa, at an altitude of approximately 3400 m, and therefore not climatologically significant. The main purpose of the mountaintop measurements was for calibration. The value for Hawaii in Table 4 is for one winter when the sun photometer was stationed

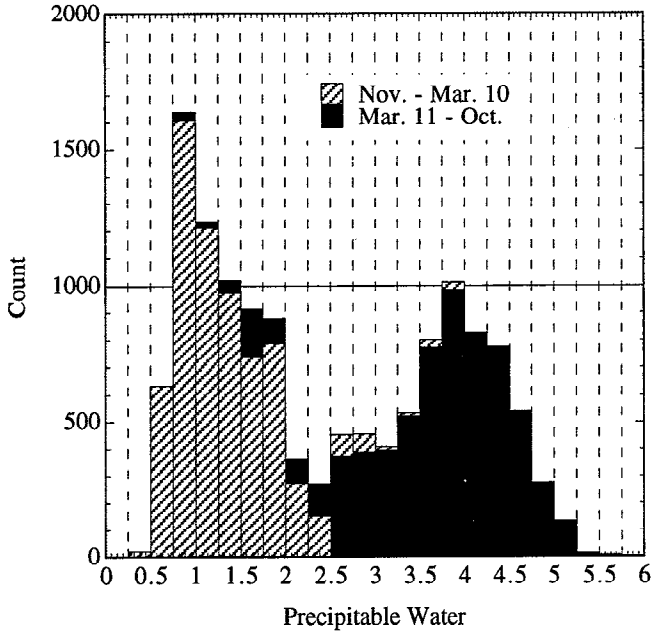

Figure 6. Histogram of precipitable water measured in Ouagadougou, Burkina Faso, in 1995. Data are recorded for all of 1995 except the month of July. Most of the low values result from North Easterly flow off the Sahara during winter months when the ITCZ is to the south. The high values result from moist Southerly flow off the Gulf of Guinea during summer, when the ITCZ is to the north.

at sea level. In the rain forest of Brazil, values are highest around 5 cm during the summer (December-February) but lower (2.9) during the winter months. As such, the winter values in the rain forest are comparable to the summer values in the midlatitude northeastern United States.

Conclusions

Atmospheric conditions alter the relationship between the transmission in the 940-nm water band and the column abundance of water vapor in the atmosphere so as to introduce a large error in the measurement of PW using sun photometers that use a large bandwidth. For those that use a narrowband width of approximately 10 nm the error due to the lack of knowledge of the atmospheric condition is shown to be less than 1%. The position of the band is not sensitive to this relationship as long as sufficient absorption occurs within the band. Thus for sun photometers that use a narrow 940-nm band to monitor water absorption (~10 nm wide), lack of adequate calibration remains the major source of uncertainty in the determination of precipitable water amount. Comparison of PW derived from radiosondes indicates agreement to within the generally accepted uncertainty in radiosonde-derived values of ±10%, especially for the narrowband channel; however, the nature of disagreement between the two methods appears systematic, raising doubts over the quality of the calibration in either or both of the methods. For the Wallops Island intercomparison the radiosonde-derived values were higher; for BOREAS and ARM CART sites, radiosonde values were generally lower. Disagreement with the microwave-derived values is of the order of 5%, consistent with the previous findings of *Reagan et al.* [1995]. The relationship among the three measurement methods did not alter appreciably when the sun photometer data were screened for thin clouds, a surprising finding. Results from the worldwide network of sun photometers deployed since 1993 show some interesting aspects: that the boreal forest is very dry throughout the year and that the Sahel region of West Africa depicts a cycle of alternating wet and dry periods depending on the position of the ITCZ during the year.

Acknowledgments. MODTRAN-3 was made available by scientists at the Hanscomb Air Force Base, Massachusetts, in particular, G. P. Anderson. Ilya Slutsker provided analyzed Cimel Sunphotometer data and suggested improvements in data analysis procedure that reduced the analysis time considerably for a large number of sun photometers. A number of investigators around the world helped in the deployment and maintenance of the sun photometers whose data are presented here. We would like to acknowledge R. Ferrare, Hughes STX Corporation, whose initiative in deploying a Cimel at the ARM site provided valuable data for intercomparison with other ARM instruments. Wallops Island radiosonde data were obtained courtesy of NASA's Mission to Planet Earth Program, via GSFC/Wallops Flight Facility. CART site radiosonde and microwave radiometer data were obtained from the Atmospheric Radiation Measurement (ARM) Program sponsored by the U.S. Department of Energy, Office of Energy Research, Office of Health and Environmental Research, Environmental Sciences Division. This research was supported [in part] by the Environmental Sciences Division of the U.S. Department of Energy (DOE) as part of the Atmospheric Radiation Measurement Program and was performed under the auspices of DOE under Contract No. DE-AC02-76CH00016.

References

Anderson, G. P., et al., MODTRAN 3: Suitability as a flux-divergence code, paper presented at Fourth Atmospheric Radiation Measurement (ARM) Science Team Meeting, U. S. Department of Energy, Charleston, S. C., Feb. 28 to March 3, 1994.

Bruegge, C. J., J. E. Conel, R. O. Green, J. S. Margolis, R. G. Holm, and G. Toon, Water vapor column abundance retrievals during FIFE, *J. Geophys. Res.*, *97* (D17), 18,759-18,768, 1992.

Ferrare, R. A., S. H. Melfi, D. N. Whiteman, K. D. Evans, F. J. Schmidlin, and D. O'C. Starr, A comparison of water vapor measurements made by Raman lidar and radiosondes, *J. Atmos. Oceanic Technol.*, *12* (6), 1177-1195, 1995.

Gaffen, D. J., and W. P. Elliott, Column water vapor content in clear and cloudy skies, *J. Clim.*, *6*, 2278-2287, 1993.

Goody, R. M., *Atmospheric Radiation*, vol. 1, *Theoretical Basis*, Clarendon, Oxford, 1964.

Halthore, R. N., B. L. Markham, and D. W. Deering, Atmospheric correction and calibration during KUREX-91, *IGARSS'92, Int. Geosci. Remote Sens. Symp.*, *2*, 1278-1280, 1992.

Holben, B. N., and T. F. Eck, Precipitable water in the sahel measured using sunphotometry, *Agric. For. Meteorol.*, *52*, 95-107, 1990.

Holben, B. N., et al., Automatic sun and sky scanning raiometer system for network aerosol monitoring, *Remote Sens. of Environ.*, in press.

Justice, C. O., T. Eck, D. Tanre, and B. Holben, The effect of water vapour on the normalized difference vegetation index derived for the Sahelian region from NOAA AVHRR data, *Int. J. Remote Sens.*, *12* (6), 1165-1183, 1991.

Kneizys, F. X., E. P. Shettle, L. W. Abreu, J. H. Chetwynd, G. P. Anderson, W. O. Gallery, J. E. A. Selby, and S. A. Clough, Users guide to LOWTRAN 7, *Tech. Rep. AFGL-TR-88-0177*, Air Force Geophys. Lab., Hanscom Air Force Base, Mass., 1988. (Available as AD A206773 from Natl. Tech. Inf. Serv., Springifeld, Va.)

Michalsky, J., C. Liljegren, and L.C. Harrison, A comparison of sunphotometer derivations of total column water vapor and ozone to statndard measures of same at the southern Great Plains atmospheric radiation measurement site, *J. Geophys. Res.*, *100* (D12), 25,995-26,003, 1995.

Pitts, D. E., W. E. McAllum, M. Heidt, K. Jeske, and J. T. Lee, Temporal variations in atmospheric water vapor and aerosol optical

depth determined by remote sensing, *J. Appl. Meteorol.*, *16*, 1312-1321, 1977.

Reagan, J., K. Thome, B. Herman, R. Stone, J. DeLuisi, and J. Snider, Intercomparisons of columnar water vapor retrievals obtained with near-IR Solar radiometers and microwave radiometers, *J. Appl. Meteorol.*, *346*, 1384-1391, 1995.

Reagan, J., K. J. Thome, and B. M. Herman, A simple instrument and technique for measuring columnar water vapor via near-IR Differential solar transmission measurements, *IEEE Trans. Geosci. Remote Sens.*, *30, 825-831*, 1992.

Reagan, J. A., P. A. Pilewskie, I. C. Scott-Fleming, B. M. Herman, and A. Ben-David, Extrapolation of earth-based solar irradiance measurements to exoatmospheric levels for broad-band and selected absorption-band observations, *IEEE Trans. Geosci. Remote Sens.*, *GE-25* (6), 647-653 1987.

Schmid, B., K. J. Thome, P. Demoulin, R. Peter, C. Mätzler, and J. Sekler, Comparison of modeled and empirical approaches for retrieving columnar water vapor from solar transmittance measurements in the 0.94-mm region, *J. Geophys. Res.*, *101* (D5), 9345-9358, 1996.

Sellers, P. J., et al., The Boreal Ecosystem-Atmosphere Study (BOREAS): an overview and early results from the 1994 field year, *Bull. Am. Meteorol. Soc.*, *76* (9), 1549-1577 1995.

Shiobara, M., J. D. Spinhirne, A. Uchiyama, and S. Asano, Optical depth measurements of aerosol, cloud, and water vapor using sun photometers during FIRE Cirrus IFO II, *J. Appl. Meteorol.*, *35*, 36-46, 1996.

Thome, K. J., B. M. Herman, and J. A. Reagan, Determination of precipitable water from solar transmission, *J. Appl. Meteorol.*, *31*, 157-165, 1992.

Volz, F. E., Economical multispectral sun photometer for measurements of aerosol extinction from 0.44 to 1.6 micron and precipitable water, *Appl. Opt.*, *13*, 1732-1733, 1974.

Wiscombe, W. J., An absorbing mystery, *Nature*, *376*, 466-467, 1996.

T. F. Eck, Hughes-STX Corporation, Lanham, MD 20706.

Rangasayi N. Halthore, Brookhaven National Laboratory, Department of Appied Science, Environmental Chemistry Division, Bldg. 426, Upton, NY 11973. (e-mail: halthore@bnl.gov)

B. N. Holben and B. L. Markham, Laboratory for Terrestrial Physics, NASA Goddard Space Flight Center, Greenbelt, MD 20771.

(Received June 17, 1996; revised September 30, 1996; accepted October 15, 1996)